

## Positron self-trapping in $\text{Nd}_2\text{Fe}_{14}\text{B}$

This article has been downloaded from IOPscience. Please scroll down to see the full text article.

1991 J. Phys.: Condens. Matter 3 2507

(<http://iopscience.iop.org/0953-8984/3/15/005>)

View [the table of contents for this issue](#), or go to the [journal homepage](#) for more

Download details:

IP Address: 171.66.16.96

The article was downloaded on 10/05/2010 at 23:06

Please note that [terms and conditions apply](#).

## Positron self-trapping in $\text{Nd}_2\text{Fe}_{14}\text{B}$

S Mäkinen, O-P Kähkönen and M Manninen

Department of Physics, University of Jyväskylä, SF-40100 Jyväskylä, Finland

Received 15 October 1990, in final form 7 January 1991

**Abstract.** The positron lifetime technique has been used to study a permanent magnet material  $\text{Nd}_2\text{Fe}_{14}\text{B}$ . It was found that at low temperatures ( $T < 125$  K) positrons are trapped in a polaron-like state at regions of low ion density in the unit cell. At higher temperatures ( $T > 175$  K), positron diffusion is fast enough for trapping into deep vacancy-type defects at the grain boundaries.

### 1. Introduction

The positron lifetime technique [1, 2] has been widely used in studying lattice defects in crystalline material. The method is very suitable for identification of open-volume defects, such as single vacancies, vacancy-impurity pairs and vacancy clusters. The trapping of positrons at these vacancy-type defects is rather strong and they are often referred as deep traps. At low temperatures, positrons can also get trapped by defects where the density of positive ion cores is only slightly lower than in the surrounding perfect crystal. In metals, dislocation lines and loops [3, 4] are the most important examples of these weak positron traps, where the binding energy of positrons is of the order of 100 meV [5, 6].

In most of the materials studied the positron mobility is large and only lattice defects provide positron traps. In a perfect crystalline material, the positron wave function is delocalized, having maximum values in the interstitial regions and being almost zero at the ion sites. This picture is true when the lattice structure is simple. However, in complicated structures the situation may be different: the unit cell might have regions where the ion density is, from the positron point of view, significantly smaller than the average value. These regions can offer self-trapping sites for positrons, which could form polaron-like states [7].

One of the materials with a complex structure is the new permanent magnet material  $\text{Nd}_2\text{Fe}_{14}\text{B}$ , which has recently been studied intensively [8, 9]. Due to the different sizes of the Nd, Fe and B atoms, the ion density is different in different parts of the unit cell. This makes possible polaron-like positron self-trapping in the bulk.

In this paper we report on positron lifetime measurements made for  $\text{Nd}_2\text{Fe}_{14}\text{B}$  at temperatures between 15 K and 300 K. The results show evidence for reduced positron mobility at low temperatures. The theoretical calculations indicate the possibility of polaron-type self-trapping in the perfect crystal.

## 2. Experimental details

### 2.1. Samples

The Nd-Fe-B alloy-based neomagnets studied in the present work are sintered permanent magnets with excellent magnetic properties and with a complex crystallographic structure [8]. The main phase in the crystal is  $\text{Nd}_2\text{Fe}_{14}\text{B}$  and the grain size in the studied samples is about 15–30  $\mu\text{m}$ . The atomic structure of a unit cell containing 68 atoms (four  $\text{Nd}_2\text{Fe}_{14}\text{B}$  units) in the main phase is shown in figure 1. All the Nd and B atoms are on the  $z = 0$  and  $z = 0.5$   $c$  planes but only four of the 56 iron atoms are on these planes. The other iron atoms form puckered, hexagonal nets which lie between the  $z = 0$  and  $z = 0.5$   $c$  planes. The lattice constants of this phase are:  $a = 8.80$  Å and  $c = 12.19$  Å. The space group of the  $\text{Nd}_2\text{Fe}_{14}\text{B}$ -phase is  $P4_2/mnm$  [8].

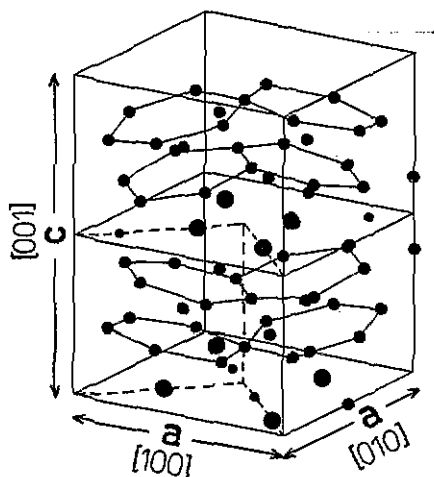


Figure 1. The atomic structure of a  $\text{Nd}_2\text{Fe}_{14}\text{B}$  unit cell. The Nd atoms are denoted by the largest shaded circles, the Fe atoms by the medium-size black circles and the B atoms by the small black circles. The computational cell used in the positron state calculations is marked by broken lines.

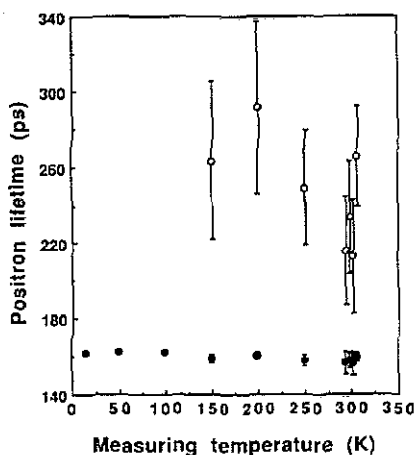


Figure 2. The positron lifetime components as a function of measuring temperature for the sintered  $\text{Nd}_2\text{Fe}_{14}\text{B}$  samples. For clarification, the four values measured at 300 K are slightly separated in the figure.

In preparing the samples, Nd-Fe-B ingots were crushed under an argon atmosphere to a particle size of less than 500  $\mu\text{m}$  and then pulverized in an inert atmosphere and in an organic fluid to a particle size of about 2–5  $\mu\text{m}$  in a ballmill. The powders were oriented in a magnetic field of about 0.8 T under 200 MPa pressure. The direction of the magnetic field was perpendicular to the pressing direction. The pressed compacts were sintered in pure argon atmosphere at 1340 K for 1 h and cooled as quickly as possible. After this the magnets were post-sintered at 850–950 K by using the same kind of procedure as in the first heat treatment. Finally, the samples were cut to appropriate dimensions by a diamond saw.

Besides the main  $\text{Nd}_2\text{Fe}_{14}\text{B}$ -phase, also other Nd-Fe-B based phases can be found in the grain boundaries of the main phase, especially in the triangles formed by the grain boundaries crossing each other. In these boundaries also the presence of open-volume defects is rather probable.

The samples used in the positron lifetime measurements were demagnetized before the measurements. The reason for this is a solely technical one: a strong magnetic field might disturb the photomultipliers used in detecting gamma quanta in the experiments. The thickness of the samples was about 0.5 mm which is enough to absorb more than 99% of the positrons emitted by the source [10].

## 2.2. Facility

The positron lifetime measurements were done by using the JYFL low-temperature facility [11]. The temperature of the samples can be adjusted to any value between 15 K and 300 K by using a two-stage helium refrigerator and a microcomputer-controlled heating system. The temperature of the sample holder is measured using a copper-constantan thermocouple. The samples are mounted in a sample-source-sample sandwich geometry to the cold-head. The  $^{22}NaCl$  positron source used in the measurements is enveloped in a thin ( $1.7 \text{ mg cm}^{-2}$ ) Havar foil.

The lifetime spectrometer consists of a plastic scintillator for the 1.275 MeV start gamma and of a  $BaF_2$  scintillator for the annihilation gamma (511 keV). Philips XMP photomultipliers are used in strengthening the pulses. The lifetime events are gathered in a multichannel analyser (MCA), and the spectra of about one million accepted events are analysed using the Fortran programs RESOLUTION and POSITRONFIT [12]. The variance of the fit was typically less than 1.25.

## 2.3. Results

The time resolution of the positron lifetime spectrometer was determined by measuring the positron lifetime in perfect single-crystal Mo at 15 K. The lifetime spectra were analysed with the Fortran program RESOLUTION [12], and the resolution function was found to be a one-component gaussian function with a FWHM of 217 ps. The lifetime components due to the positron source were also determined by this program. It was found that the total intensity of the source components was 17.8% with lifetimes of 170 ps (14.6%) and 380 ps (3.2%) due to the Havar foil and the  $^{22}NaCl$  salt, respectively.

The positron lifetimes in the  $Nd_2Fe_{14}B$  samples were measured at temperatures between 15 K and 300 K, and the lifetime spectra were analysed by using the Fortran program POSITRONFIT [12]. At 15 K, only one lifetime component could be detected:  $\tau \approx 162$  ps (figure 2). The analysis failed drastically if one tried to separate two lifetimes in the spectra. However, the analysis of the positron lifetime spectra measured at room temperature clearly resulted in two components:  $\tau_1 \approx 157$  ps and  $\tau_2 \approx 230$  ps (figure 2). The long lifetime component was most probably due to positrons trapped at vacancy-type defects in the grain boundaries. The intensity of the second component was about 12% at 300 K (figure 3). Although the statistical error bars seem to be quite large, it was impossible to find a good fit with only one lifetime component in the analysis.

The positron lifetime spectra were also measured at 50–250 K (figures 2 and 3). Only one lifetime component could be separated in the spectra measured at 50 K and at 100 K, whereas at 200–250 K two lifetime components could clearly be separated in the spectra. The results for the lifetime spectra measured at 125 K and at 150 K seem to be indistinct: both one-component and two-component analysis gave somewhat reasonable results for the 125 K spectrum, but with very large error bars in  $\tau_2$ . One of the two spectra measured at 150 K gave a rather good fit for only one lifetime,

while the analysis for the other spectrum resulted in two lifetime components. It thus seems that the temperature of about 150 K divides the trapping of positrons into two groups: at temperatures below 125 K only one type of traps are possible for positrons, whereas above 175 K two kinds of positron traps are clearly present.

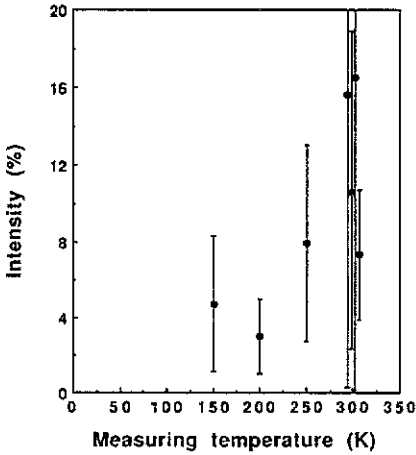


Figure 3. The intensity of the second lifetime component,  $I_2$ , versus measuring temperature. The values at 300 K are separated in the figure.

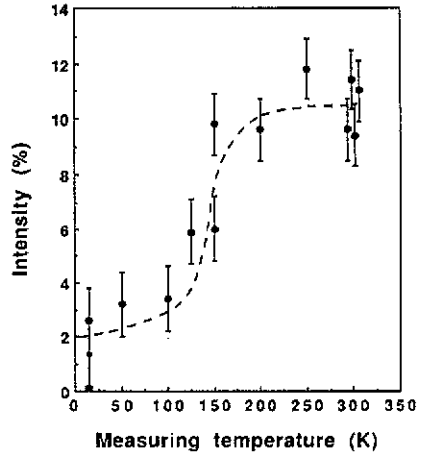


Figure 4. The intensity of the long lifetime component fixed to 230 ps in the analysis of the positron lifetime spectra.

In order to study the behaviour of the intensity of the defect-related lifetime component,  $I_2$ , the value of  $\tau_2$  was fixed to its mean value at 300 K, 230 ps. The results of the two-component analysis are shown in figure 4. The figure supports the conclusion about the presence of only one kind of positron traps below 125 K and two kinds of traps above 175 K.

The sudden increase in  $I_2$  at a rather high temperature can be explained by the presence of shallow positron traps, which prevent the positron diffusion into the deep traps. Dislocation lines and loops are known to be shallow positron traps in metals [5, 6, 13]. Our theoretical considerations in the next section show that in the case of  $\text{Nd}_2\text{Fe}_{14}\text{B}$  there is also another possibility: due to the complex atomic structure, a polaron-like self-trapping becomes possible.

### 3. Theory

#### 3.1. Calculation method

The possibility of positron self-trapping in the  $\text{Nd}_2\text{Fe}_{14}\text{B}$  crystal was theoretically studied by calculating the positron wave function and annihilation rate in a perfect neomagnet lattice. The calculations were done by using a well-tested method [14–16] which uses atomic superposition in determining the three-dimensional electron density and electrostatic potential in the host. In the calculations, atoms are fixed to sites corresponding to the given lattice structure. The coordinates used for the Nd, Fe and B atoms are taken from [8], where the values have been determined by the neutron-diffraction method. Due to the absence of thermal energy in the calculations,

the calculated positron state corresponds to the low-temperature positron lifetime measurements.

For each atom (Nd, Fe and B), the values of the Coulomb potential and electron density used in the superposition were calculated by using the density functional theory [17] with a Ceperley–Alder exchange–correlation potential [18]. In these calculations the core electrons, valence electrons, and d-valence electrons are treated separately. In deciding which electrons should be taken as tightly bound core electrons, the orbital parameters calculated by Fraga *et al* [19] were used. In the case of Nd, only the two 6s electrons were treated as valence electrons while the other were handled as core electrons. For Fe the electrons in the 4s orbital, and for B the 2s and 2p electrons were treated as valence electrons in the calculations (the d-electrons in Fe were treated as core electrons).

The obtained free Nd, Fe and B atoms were placed on their lattice sites in the unit cell and the electron density  $n^-$  as well as the Coulomb potential  $V_C$  sensed by the positron were determined by summing the values of these over the whole calculation cell

$$n^-(\mathbf{r}) = \sum_i n_{at,j}^-(|\mathbf{r} - \mathbf{R}_i|) \quad V_C(\mathbf{r}) = \sum_i V_{at,j}(|\mathbf{r} - \mathbf{R}_i|). \quad (1)$$

Here  $n_{at,j}^-(r)$  and  $V_{at,j}(r)$  are the spherically symmetric free electron density and Coulomb potential obtained for a free atom of type  $j$  (Nd, Fe or B) at distance  $r$ , respectively. The three-dimensional atom sites are marked as  $\mathbf{R}_i$  in the equation.

The positron potential  $V_+$  used in the Schrödinger equation consists of the Coulomb part of (1) and a correlation potential  $V_{corr}$  due to the electron–positron interactions. The formula for  $V_{corr}$  is obtained by using the many-body calculations of Arponen and Pajanne for a positron in a homogeneous electron gas [20].

The positron annihilation rate with core electrons and with valence electrons is calculated by using local enhancement

$$\lambda = \pi r_0^2 c \int d\mathbf{r} |\Psi(\mathbf{r})|^2 [n_v(\mathbf{r})\gamma_v(n_v(\mathbf{r})) + n_c(\mathbf{r})\gamma_c]. \quad (2)$$

Here  $r_0$  is the classical electron radius,  $c$  is the speed of light,  $n_v$  and  $n_c$  are the valence and core electron densities, and  $\gamma_v$  and  $\gamma_c$  are the enhancement factors for the valence and core electrons, respectively. The formula of Brandt and Reinheimer [21] was used for  $\gamma_v$  and a value of 1.5 for  $\gamma_c$ . The positron lifetime,  $\tau$ , is the inverse of  $\lambda$ .

### 3.2. Results

The volume of the computational cell could be reduced to one eighth of the unit cell by using the structural symmetries of the lattice (see figure 1). In determining the electron density and the electrostatic potential inside the cell, the contribution of the atoms outside the cell was also taken into account in the superposition. In calculating the positron wave function, mirror-symmetry boundary conditions were used at both walls in the  $\langle 001 \rangle$  and in the  $\langle 110 \rangle$  directions. At the  $\langle 010 \rangle$  wall we made use of the inversion symmetry with respect to the vertical line in the centre of this wall. With these boundary conditions the calculated positron state corresponds to a delocalized positron in the bulk of single-crystal  $Nd_2Fe_{14}B$ .

The positron potential was first calculated at nodes of a three-dimensional net forming an orthorhombic Bravais lattice in the calculation cell. The separation between two adjacent nodes was 0.176 Å in the  $\langle 100 \rangle$  and in the  $\langle 010 \rangle$  directions and

0.179 Å in the  $\langle 001 \rangle$  direction. The Schrödinger equation was discretized, and it was solved at the node points by using a relaxation method. A constant value of 0.1 was used for the initial value of the positron wave function at every calculation point. The wave function was relaxed to a form which minimizes the energy eigenvalue of the positron. The relaxation was tested by using also a cosine-like initial wave function in starting the relaxation. When about 5000 iteration loops were used, no changes could be seen in the final form of the wave functions calculated using these two initial values, and also the positron lifetime and the energy eigenvalue were the same within 0.4 ps and 3 meV, respectively.

A contour plot of the relaxed positron wave function is shown in figure 5 at the diagonals of the unit cell in the  $\langle 110 \rangle$  directions. The positron is clearly localized in the regions of low ion density in the unit cell. It is interesting to note that the value of the positron wave function is, due to the atomic structure, practically zero in the middle of the unit cell. It should also be noted that the two maxima in the  $[1\bar{1}0]$  direction are located in the middle of the unit cell while the other two in the  $[110]$  direction are at the corners of the cell. This is due to the complicated symmetry of the lattice. The same kind of structure in the positron wave function is also seen when viewed from the  $\langle 001 \rangle$  direction, and at the  $\langle 010 \rangle$  wall of the unit cell.

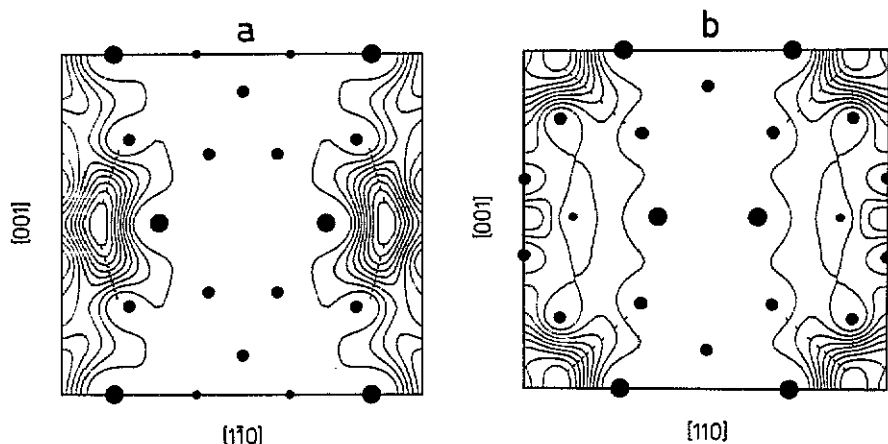


Figure 5. Contour plots of the positron wave function in the bulk of  $\text{Nd}_2\text{Fe}_{14}\text{B}$  crystal. In (a) the values of the wave function are plotted at the diagonal of the unit cell in the  $[1\bar{1}0]$  direction and in (b) in the  $[110]$  direction.

The calculated positron lifetime in the bulk state is 177 ps, in fairly good agreement with the experimental value. It is interesting to observe that this lifetime is about 70 ps longer than the bulk lifetime in iron, but about the same as the positron vacancy lifetime in iron. This means that the  $\text{Nd}_2\text{Fe}_{14}\text{B}$  crystal has interstitial sites with low electron density, and suggests that the positron could be fairly well localized in the interstitial sites.

By changing the boundary conditions for the positron Schrödinger equation we have calculated the positron energy at the Brillouin zone boundaries in the  $\langle 110 \rangle$  and  $\langle 001 \rangle$  directions. The results give an estimate of 0.2 eV for the width of the positron band, which is only about 20% of the free particle band width. The small band width is an indication that the positron can get self-trapped in the interstitial state and

form a polaron-like state. To further examine this we have computed the volume dependence of the positron energy in the delocalized state to be

$$E_d = V \frac{dE_0}{dV} \approx -11 \text{ eV} \quad (3)$$

where  $V$  is the volume of the unit cell and  $E_0$  is the bottom of the positron band. The quantity  $E_d$  is the positron deformation potential, defined in [22]. We can estimate from (3) that a change of only 2% in the volume, or 0.6% in the relaxation of the atoms nearest to the positron is needed for the positron energy eigenvalue to drop 0.2 eV, i.e., the band width. Since the energy needed for such small lattice relaxations is very small [23] we can conclude that in  $\text{Nd}_2\text{Fe}_{14}\text{B}$  the positron ground state is a polaron-like state. The accurate determination of the polaron formation energy would require self-consistent computations with the knowledge of interatomic (preferentially many-atom) interactions in  $\text{Nd}_2\text{Fe}_{14}\text{B}$ .

The polaron motion is strongly temperature dependent [24, 25]. At low temperatures the diffusion constant is proportional to  $T^7$  and at high temperatures it is governed by classical trapping and increases exponentially with temperature. It is difficult to estimate which behaviour is dominant in our experiments. However, in any case the diffusion constant is strongly  $T$ -dependent and becomes very small at low temperatures. This explains our experimental findings that with increasing temperature more and more positrons get trapped at the existing defects at the grain boundaries.

The small grain size makes it possible that a significant part of the positrons can get trapped at vacancy-type defects at grain boundaries. If the grains were round with average size of 22  $\mu\text{m}$  and if the positron diffusion length was 0.1–0.2  $\mu\text{m}$  (a typical value for a metal), about 3–6% of positrons could diffuse to the grain boundaries during their lifetime. However, the grains are always polygonal which increases the surface to volume ratio increasing the number of trapped positrons. This is in agreement with the room temperature measurements where the intensity of the longer lifetime is about 10%. However, the positron diffusion length even at higher temperatures is expected to be smaller than that for a typical metal, suggesting the existence of deep traps also inside the grains.

#### 4. Conclusions

A permanent magnet material,  $\text{Nd}_2\text{Fe}_{14}\text{B}$ , has been studied by the positron lifetime technique. Two positron lifetime components are seen in experiments above 175 K, and only one lifetime at temperatures below 125 K. Theoretical calculations on positron states in a perfect  $\text{Nd}_2\text{Fe}_{14}\text{B}$  crystal show that the positron forms a polaron-like self-trapped state in the low-ion-density regions of the unit cell. The strong temperature dependence of the polaron state allows the positron trapping in vacancies at the grain boundaries only at elevated temperatures, in agreement with the experimental results.

#### Acknowledgment

The authors would like to thank M Talvitie for preparing the  $\text{Nd}_2\text{Fe}_{14}\text{B}$  samples.



## References

- [1] Hautojärvi P (ed) 1979 *Positrons in Solids (Topics in Current Physics 12)* (Heidelberg: Springer)
- [2] Brandt W and Dupasquier A (ed) 1983 *Positron Solid State Physics (Proc. Enrico Fermi Int. Sch. of Physics, Course LXXXIII)* (Amsterdam: North-Holland)
- [3] Hull D and Bacon D J 1984 *Introduction to Dislocations* (Oxford: Pergamon)
- [4] Nabarro F R N (ed) 1979 *Dislocations in Solids* (Amsterdam: North-Holland)
- [5] Häkkinen H, Mäkinen S and Manninen M 1990 *Phys. Rev. B* **41** 12441
- [6] Mäkinen S, Häkkinen H and Manninen M 1990 *Phys. Scr. T* **33** 206
- [7] Seeger A 1985 *Positron Annihilation* ed P C Jain, R M Singru and K P Gopinathan (Singapore: World Scientific) p 48
- [8] Herbst J F, Croat J J, Pinkerton F E and Yelon W B 1984 *Phys. Rev. B* **29** 4176
- [9] Jaswal S S 1990 *Phys. Rev. B* **41** 9697
- [10] Linderoth S, Hansen H E, Nielsen B and Petersen K 1984 *Appl. Phys. A* **33** 25
- [11] Hansen H E, Talja R, Rajainmäki H, Nielsen H K, Nielsen B and Nieminen R M 1985 *Appl. Phys. A* **36** 81
- [12] Kirkegaard P, Eldrup M, Mogensen O E and Pedersen N J 1981 *Comput. Phys. Commun.* **23** 307
- [13] Linderoth S and Hidalgo C 1987 *Phys. Rev. B* **36** 4054
- [14] Puska M J and Nieminen R M 1983 *J. Phys. F: Met. Phys.* **13** 333
- [15] Puska M J 1987 *Phys. Status Solidi a* **102** 11
- [16] Jensen K O, Nieminen R M and Puska M J 1989 *J. Phys.: Condens. Matter* **1** 3727
- [17] Lundqvist S and March N H 1983 *Theory of the Inhomogeneous Electron Gas* (New York: Plenum)
- [18] Ceperley D M and Alder B J 1980 *Phys. Rev. Lett.* **45** 566  
Vosko S H, Wilk L and Nusair M 1980 *Can. J. Phys.* **58** 1200
- [19] Fraga S, Saxena K M S and Karwowski J 1976 *Handbook of Atomic Data* (Amsterdam: Elsevier Scientific)
- [20] Arponen J and Pajanne E 1979 *Ann. Phys., NY* **121** 343; 1979 *J. Phys. F: Met. Phys.* **9** 2359
- [21] Brandt W and Reinheimer J 1971 *Phys. Lett.* **35A** 109
- [22] Puska M J, Lanki P and Nieminen R M 1989 *J. Phys.: Condens. Matter* **1** 6081
- [23] Puska M J and Nieminen R M 1984 *Phys. Rev. B* **29** 5382
- [24] Holstein T 1959 *Ann. Phys., NY* **8** 325
- [25] Flynn C P and Stoneham A M 1970 *Phys. Rev. B* **1** 3966